

Transport in gapped bilayer graphene: the role of potential fluctuations

Ke Zou and Jun Zhu

Department of Physics, The Pennsylvania State University, University Park, PA 16802-6300

Online Supporting Information

1. The energy and size distribution of electron and hole puddles in bilayer graphene.
2. The calculation of $\langle \varepsilon_{ij} \rangle$.
3. Raman spectra on dual-gated bilayer graphene.

1. The energy and size distribution of electron and hole puddles in bilayer graphene:

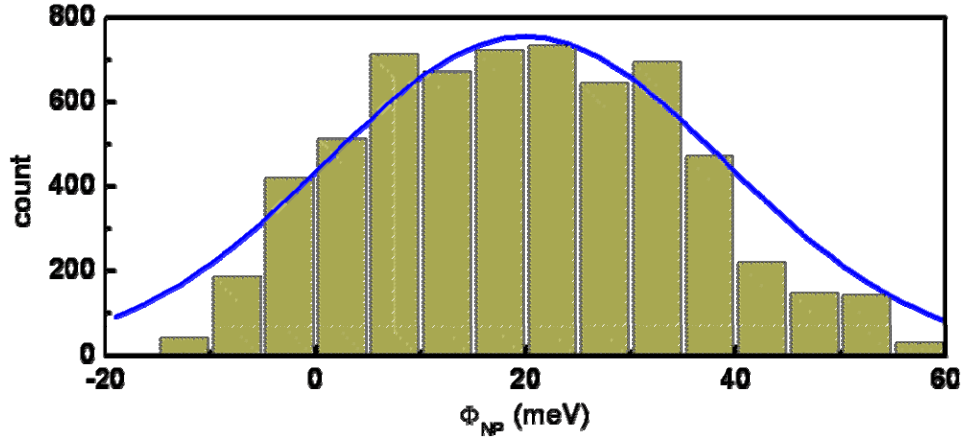


Figure S1. The histogram of Φ_{NP} in Fig. 3 of Ref. 1. The blue solid line is a Gaussian fit.

Figure S1 plots a histogram of the charge neutrality point (CNP) potential Φ_{NP} of bilayer graphene on SiO_2 , extracted from scanning tunneling spectroscopy data reported in Fig. 3 of Ref. 1. The solid line is a Gaussian fit which yields $\Phi_{NP} = (20 \pm 19)$ meV.

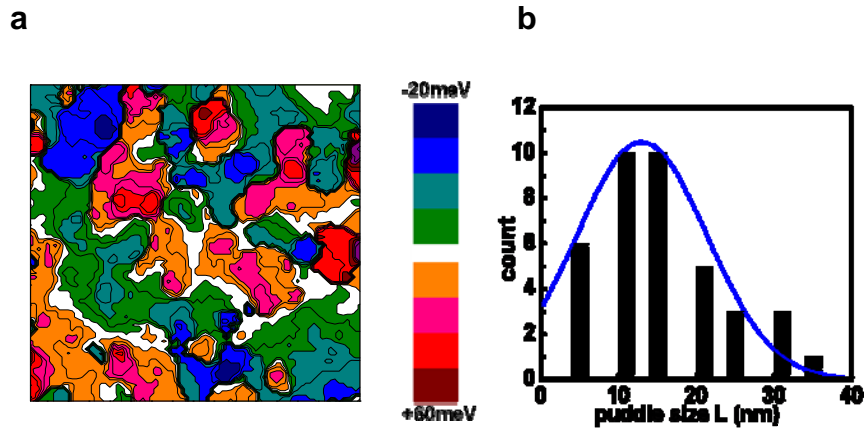


Figure S2: (a) Φ_{NP} data in Fig. 3 of Ref. 1. The map is 80 x 80nm. Each color represents a 10 meV step. (b) The histogram of puddle size L from (a). The blue solid line is the best fit by a Gaussian distribution and yields $L = (13 \pm 8.4)$ nm.

Figure S2 (a) shows the spatial map of the same Φ_{NP} data in a false color plot. The white area corresponds to 20 ± 2.5 meV, representing a small gap separating electron

and hole puddles. We approximate each puddle as a polygon and estimate the lateral size L . Puddles of the same carrier type separated by a barrier of less than 5 meV are joined together and counted as one large puddle. The histogram of L obtained from both electron and hole puddles and from both dimensions is shown as Fig. S2 (b). A truncated and normalized Gaussian fit yields a distribution of

$$P(L) = \frac{1.06}{\sqrt{2\pi\sigma^2}} \exp\left(-\frac{(L - L_0)^2}{2\sigma^2}\right), \quad (1)$$

where $L_0 = 13$ nm and $\sigma = 8.4$ nm for $L > 0$ and $P(L)=0$ for $L \leq 0$.

2. The calculation of $\langle \varepsilon_{ij} \rangle$:

We simplify the fluctuating potential as a network of cylindrical potential wells with a fixed depth V_0 but varying size L (Fig. 5(a) in the text and Fig. S3) and solve for the eigenenergies of the bound states for different L . The resulting $\varepsilon_i(L)$ for $V_0 = 13$ meV and 43 meV are shown in Fig. 5 (b) of the text.

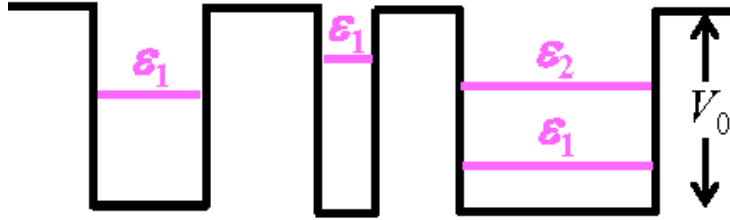


Figure S3. Localized states in cylindrical potential wells. A narrower well has a higher ground state energy and a wider well may have more than one bound state.

The average energy difference between neighboring states $\langle \varepsilon_{ij} \rangle$ is calculated using the following equation:

$$\langle \varepsilon_{ij} \rangle = \langle |\varepsilon_i(L_i) - \varepsilon_j(L_j)| \rangle = \iint_{L_i, L_j} |\varepsilon_i(L_i) - \varepsilon_j(L_j)| P(L_i) P(L_j) dL_i dL_j. \quad (2)$$

For wells with 2 bound states, the 1st excited state is used in the calculation.

3. Raman spectra on dual-gated bilayer graphene.

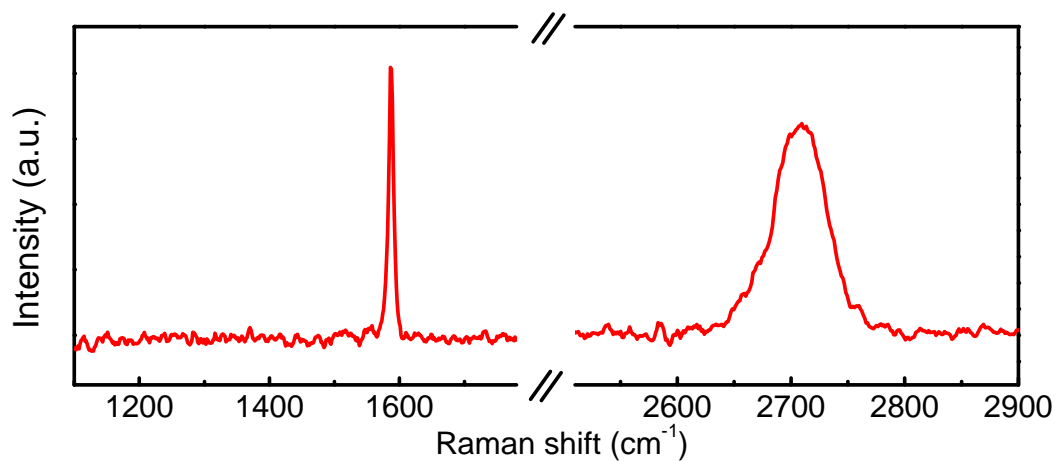


Figure S4. Raman spectra on sample A1 taken with 514 nm laser excitation. The horizontal axis scale is different for the G (1580 cm⁻¹) and 2D (~ 2700 cm⁻¹) regions.

Figure S4 shows a Raman spectrum taken on sample A1. The spectrum shows the characteristic 2D band of bilayer graphene. No visible D band (1360cm⁻¹) is observed.

¹ A. Deshpande, W. Bao, Z. Zhao, C. N. Lau, and B. J. LeRoy, *Appl. Phys. Lett.* **95**, 243502 (2009).